High-performance liquid chromatography/high-resolution mass spectrometry for the characterization of transformation products of ionic liquids

(Article begins on next page)

07 January 2023

1   **HPLC-HRMS for the characterization of transformation products of ionic liquids.**

2   Debora Fabbri[1], Paola Calza*[1], Giorgio Noè[1], Valentina Santoro[2], Claudio Medana[2]

3   [1] Department of Chemistry, University of Torino, via P. Giuria 5, 10125 Torino, Italy.

4   [2] Department of Molecular Biotechnology and Health Sciences, University of Torino, via P. Giuria 5,

5   10125 Torino, Italy.

6   *corresponding author: paola.calza@unito.it

7

8   **Abstract**

9   RATIONALE

10   Ionic liquids (ILs) are a subject of active research in the field of alternative solvents. We studied the

11   behaviour of a piperidine IL, 1-butyl-1-methylpiperidinium tetrafluoroborate (BMPA), through the

12   elucidation of its transformation products (TPs) in water.

13   METHODS

14   The transformation pathways of BMPA were investigated using high-performance liquid

15   chromatography (HPLC) combined with a hybrid LTQ-Orbitrap instrument on the basis of mass

16   defect filtering. BMPA transformation products were identified by fragmentation patterns and

17   accurate mass measurements.

18   RESULTS

19   The separation and identification of 32 TPs was achieved. BMPA can be oxidized at different

20   positions in the alkyl chains. The ultimate products corresponds to N-methylpiperidinium and some

21   byproducts involving ring-opening. Tests of acute toxicity, evaluated with *Vibrio Fischeri* bacteria,

22   show that BMPA transformation proceeds through the formation of slightly harmful compounds.

23   CONCLUSIONS

24   Results showed that the main transformation pathways of BMPA were alkyl chain

25   hydroxylation/shortening and de-alkylation, and that HPLC/LTQ-Orbitrap can serve as an important

26   analytical platform to gather the ILs unknown transformation products.

27

INTRODUCTION

Ionic liquids (ILs) are a subject of active research in the field of alternative solvents, being promoted as "green chemistry" replacements to traditional solvents used in industry [1]. The great interest toward these compounds relies on their attractive properties such as low vapour pressures and flammability, chemical and thermal stability, high ionic conductivity, wide electrochemical potential window and ability to behave as catalysts [2-4].

Only few studies have reported on ILs environmental fate [5]. Photochemistry is a potentially important attenuation route influencing ILs fate in surface waters [6,7]. Although there is limited environmental data about these compounds, the low biodegradability [8] and considerable ecotoxicity of some of them underscore the importance to prevent ILs leakage into the environment and to develop effective means of removal and recovery from wastewaters [2,9,10]. Recently, several studies describe the use of advanced oxidation processes towards ILs decomposition [2,11-15], while data on the identification of their transformation product are scarce [16,12] and chiefly concerning imidazolium ILs [17].

In this work, we focus on piperidinium ILs that, next to imidazolium, are the most popular and versatile ILs.

The literature indicates that piperidinium based ionic liquids offer advantages over imidazolium ionic liquids such as strong hydrophobicity, fast phase disengagement, and economical. In view of this piperidinium ionic liquid based solvent systems have been used for the extraction of actinides, such as uranium [18] and thorium [19], showing more efficiency than the conventional imidazolium based system.

A previous (recent) study examined the desulfurization ability of three alkyl-piperidinium-based ionic liquids (PIPILs) from heptane, which was used as a model of gasoline and diesel oils [20].

Furthermore, piperidinium trifluoroacetate (PPHTFA) ionic liquid has been employed as catalyst for activation of hydrogen peroxide (H_2O_2) for selective oxidation of thioanisole to its corresponding sulfoxide at room temperature [21]. In the work of Maan Hayyan et al. for the first time a piperidinium and pyrrolidinium based ILs were used as media for the chemical generation of superoxide ion, $O_2^{\bullet-}$, by dissolving KO_2 for the destruction of chlorobenzenes at ambient conditions [22].

It should be pointed out that ionic liquids based on piperidinium cations exhibit enhanced electrochemical stability when compared to their imidazolium and pyrrolidinium homologues, which makes them interesting electrolytes for the electrodeposition of hardly reducible elements such as rare-earth [23].

In this field, recently synthesized N-alkyl-N-methylpiperidinium ionic liquids have proved to be potentially useful for electrochemical systems due to their water immiscibilities, high conductivities, electrochemical windows, high thermal stability, which is crucial with regard to safety. For example, 1-methyl- 1-

63 butylpiperidinium bis(trifluoromethylsulfonyl)imide improves the stabilization of the chemical composition

64 and structure of the sulfur cathode in Li/S cells during charge–discharge cycles [24].

65 Some piperidinium compounds were screened for their biodegradability by Neumann et al. [25] and

66 have shown a similar recalcitrance to biodegradation; only few were fully mineralized [25-27]. The

67 n-propyl alcohol substituted IL, was the only derivative from this group to be classified as readily

68 biodegradable.

69 The aim of this work was to study the behaviour of 1-butyl-1-methylpiperidinium tetrafluoroborate

70 (BMPA), through the characterization of its transformation products (TPs) in water. The separation

71 and identification of TPs is a crucial aspect because, in addition to provide important information

72 on the mechanism of degradation, they may have a very different impact on the environment

73 compared to the parent molecules. Moreover the global ionic liquid market is expected to reach

74 USD 62.3 million by 2025 because these solvents comply with the environmental norms laid down

75 by Registration, Evaluation, Authorisation and Restriction of Chemicals (REACH) which in turn is

76 positively impacting the industry [28]. It is hence extremely important to have tools to monitor the

77 presence of methylpyridinium ionic liquids transformation products in the environment.

78 However, this task is not easily achievable as a complex mixture of transformation products

79 containing isobaric species, difficult to discriminate and separate, can be formed. In a previous

80 study, some TPs were identified during BMPA degradation *via* micro-electrolysis system [29]. Here

81 we were able to follow the evolution of a larger number of TPs and to discriminate several isobaric

82 species, employing HPLC-HRMS using a hybrid LTQ-Orbitrap analyzer.

83

84

EXPERIMENTAL SECTION

Materials and Reagents

87 1-Butyl-1-methylpiperidine tetrafluoroborate (BMPA) (99%), acetonitrile (≥99.9%), formic acid

88 (99%) and phosphoric acid were purchased from Sigma Aldrich, Milan, Italy. All aqueous solutions

89 were prepared with ultrapure water Millipore Milli-Q^{TM}.

90 TiO$_2$ P25 (Evonik Industries, Pandino, Italy) was used as photocatalyst, after being subjected to

91 irradiation and washings with ultrapure water in order to eliminate the potential interference

92 caused by adsorbed ions such as chloride, sulfate and sodium. In all photocatalytic experiments,

93 TiO$_2$ was used at a loading of 200 mg L^{-1}.

Irradiation procedures

Irradiation experiments were performed in stirred cylindrical closed Pyrex cells (40 mm i.d. x 25 mm) on 5 ml of aqueous dispersions containing 20 mg L^{-1} of BMPA and 200 mg L^{-1} of TiO$_2$. A Blacklight Philips TLK 05 (40W) lamp source with emission maximum at 360 nm was employed for irradiation. The dispersions were collected from the cells at the end of the programmed irradiation period and then were filtered through 0.45 μM Millex LCR hydrophilic PTFE membranes (Millipore, Milan, Italy) before the analysis.

Analytical procedures

All samples were analyzed by HPLC/HRMS. The chromatographic separations, monitored using an MS analyzer, were carried out with a Phenomenex Gemini NX C18 (2) 150 × 2.1 mm × 3 μm particle size (Phenomenex, Bologna, Italy), using an Ultimate 3000 HPLC instrument (Dionex, Thermo Scientific, Milan, Italy). The Injection volume was 20 μL and the flow rate 200 μL min^{-1}. A gradient mobile phase composition was adopted, going from 5/95 acetonitrile heptafluorobutanoic acid (5 mM in water) to 25/75 in 15 min, followed by a second gradient step up to 95/5 in 27 min.

A LTQ Orbitrap mass spectrometer (Thermo Scientific, Milan, Italy) equipped with ESI ion source was used. The LC column effluent was delivered into the ion source using nitrogen as both sheath and auxiliary gas. The capillary voltage and tube lens voltage in the ESI source were maintained at 28 V and 70 V, respectively. The source voltage was set to 3.5 kV (in both positive and negative ion mode). The capillary temperature was maintained at 270°C. The acquisition method used was optimized beforehand in the tuning sections for the parent compound (capillary, magnetic lenses and collimating octapole voltages) to achieve maximum sensitivity. Mass accuracy of recorded ions (vs calculated) was ± 5 millimass units (mmu, without internal calibration).

Analyses were run using full scan MS (50-1000 *m/z* range), MS^2 acquisition in the positive ion mode, with a resolution of 30000 (500 *m/z* FWHM) in FTMS (full transmission) mode. The ions submitted to MS^2 acquisition were chosen on the base of full MS spectra abundance without using automatic dependendent scan. Collision energy was set to 30 % for all of the MS^2 acquisition methods. MS^2 acquisition range was between the values of ion trap cut-off and *m/z* of the (M+H)$^+$ ion. Xcalibur (Thermo Scientific, Milan, Italy) software was used both for acquisition and data analysis.

A Dionex instrument equipped with a conductimeter detector was used to follow the evolution of ionic inorganic degradation products. Anions were analysed with an AS9HC column and K$_2$CO$_3$ (9

126 mM) as eluent at a flow rate of 1 mL min^{-1}. Under these conditions, the retention times for nitrite

127 and nitrate were 6.83 and 9.51 min, respectively. For the cations, a C12A column was employed,

128 using methansulphonic acid (20 mM) as eluent at flow rate of 1 ml min^{-1}. In such conditions, the

129 retention time of ammonium ion was 4.7 min.

130 Total organic carbon (TOC) was measured in filtered suspensions using a Shimadzu TOC-5000

131 analyzer (catalytic oxidation on Pt at 680°C). The calibration was performed using potassium

132 phthalate standards.

133 The toxicity of reaction mixtures collected at different irradiation times was evaluated with a

134 Microtox Model 500 Toxicity Analyzer (Milan, Italy). Acute toxicity was evaluated with a

135 bioluminescence inhibition assay using the marine bacterium *Vibrio fischeri* by monitoring changes

136 in the natural emission of the luminescent bacteria when challenged with toxic compounds. Freeze-

137 dried bacteria, reconstitution solution, diluent (2% NaCl) and an adjustment solution (non-toxic 22%

138 sodium chloride) were obtained from Azur (Milan, Italy). Samples were tested in a medium

139 containing 2% sodium chloride, in five dilutions, and luminescence was recorded after 5, 15, and 30

140 min of incubation at 15°C. Since no substantial change in luminescence was observed between 5

141 and 30 minutes, only the percent toxicity recorded at 15 minutes will be discussed. Inhibition of

142 luminescence, compared with a toxic-free control to give the percentage inhibition, was calculated

143 following the established protocol using the Microtox calculation program.

144

RESULTS AND DISCUSSION

Mass fragmentation for BMPA

147 BMPA was detected at 156.1753 *m/z* in ESI positive mode. The product ions of BMPA are

148 summarized in Table 1, while MS^2 spectrum and fragmentation pathways are proposed in Figure 1.

149 The main product ions at 100.1122 and 98.0966 *m/z* were formed through the loss of a butene or

150 butane molecule. These characteristic losses will be considered in identifying the unknown

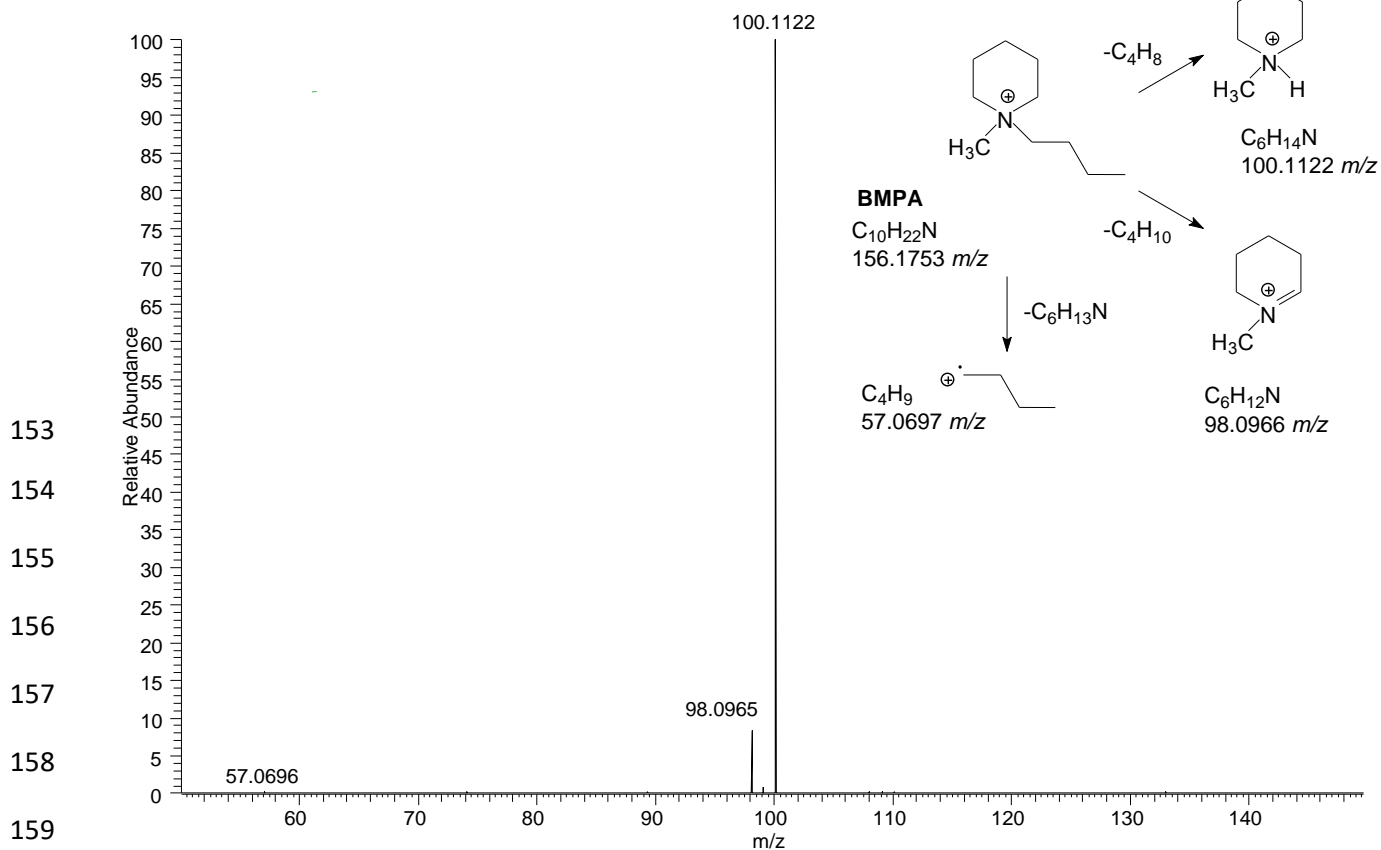151 transformation products recognized during the BMPA degradation.

152

153

154

155

156

157

158

159

100.1122

98.0965

57.0696

Relative Abundance

m/z

BMPA
$C_{10}H_{22}N$
156.1753 *m/z*

$-C_4H_8$

$C_6H_{14}N$
100.1122 *m/z*

$-C_4H_{10}$

$-C_6H_{13}N$

C_4H_9
57.0697 *m/z*

$C_6H_{12}N$
98.0966 *m/z*

160 **Figure 1**. MS^2 spectrum and proposed fragmentation pathways for BMPA.

161

162 **LC/MS analysis of BMPA transformation products**

163 BMPA photocatalytic degradation occurred within 45 min and shows the formation of thirty-two

164 transformation products (TPs) summarized in Table 1, while their MS^n ions are collected in Table S1.

165 A selection of TPs evolution profiles over time are shown in Figure 2, while the others are collected

166 in Figure S1 as supplementary information.

167

168
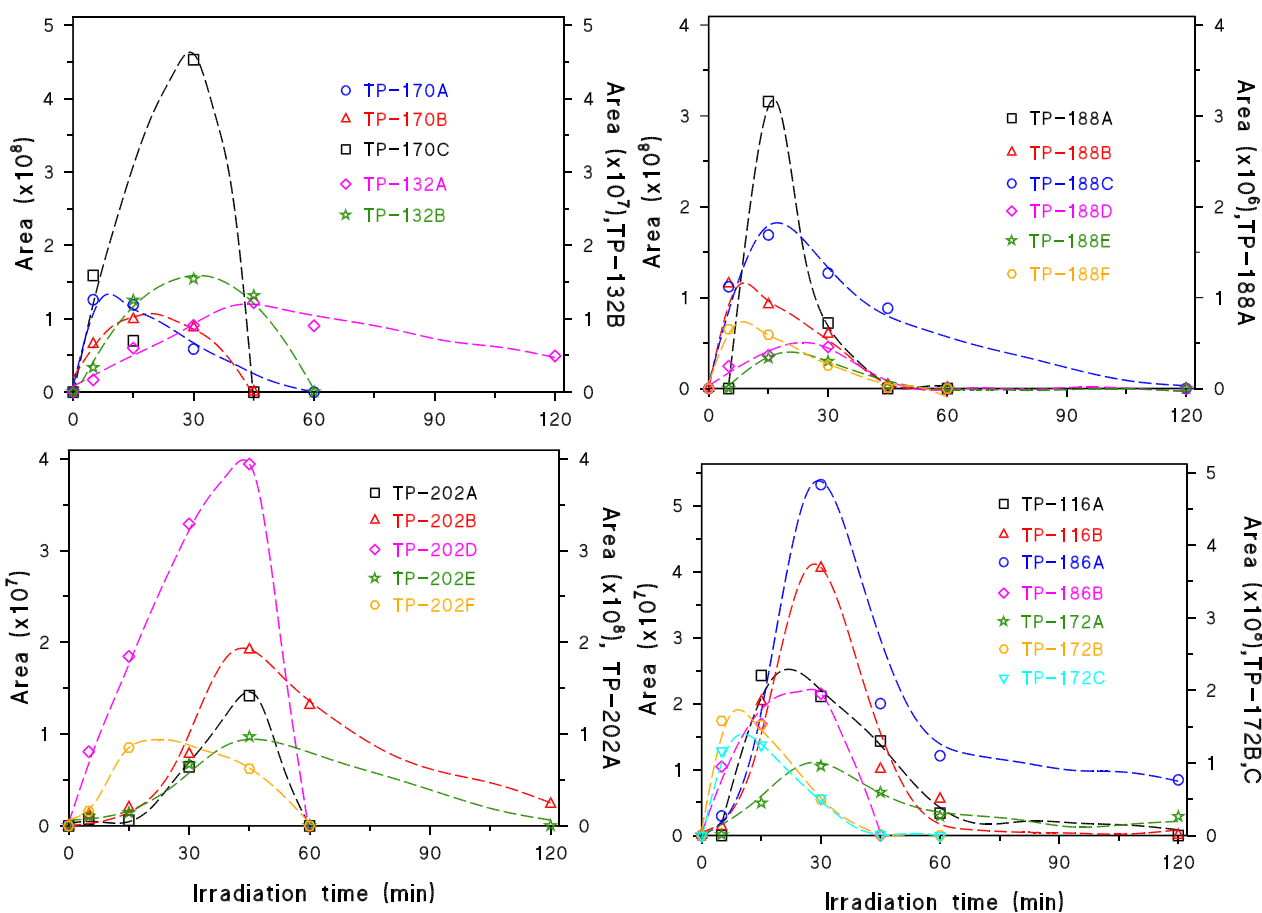
Figure 2. Transformation products formed from BMPA degradation in the presence of TiO_2

Even if TPs exhibit different kinetic evolution, most of them show a typical bell-shaped profile reaching the maximum amount within 60 min. **TP-202C** is present at trace level and, for such the time evolution is not shown. Almost all TPs were completely disappeared after two hours of irradiation.

Structural elucidation by HPLC/LTQ-Orbitrap-MS

Three TPs with 172 *m/z* are formed, whose MS^2 spectra are shown in Figure 3 and they are attributed to hydroxyl derivatives, in analogy with previously detected TPs [29]. HR-MS permits assessing two different empirical formula to these TPs. The first one (**TP-172-A)** holds 172.1334 *m/z* and an empirical formula $C_9H_{18}O_2N$, well matched with a demethylation, monohydroxylation and oxidation. MS^2 spectrum allows locating an hydroxyl group on the pyridine and the carbonyl on C2 chain position. **TPs-172-B** and **C** hold 172.1705 *m/z*, with an empirical formula $C_{10}H_{16}ON$ and are recognized as the monohydroxylated derivatives. The presence of a product ion at 100.1102 *m/z* in

184   their MS^2 spectra, due to the loss of a hydroxybutane radical ion, allows locating the hydroxyl on

185   the butyl chain, in agreement with literature data [29].
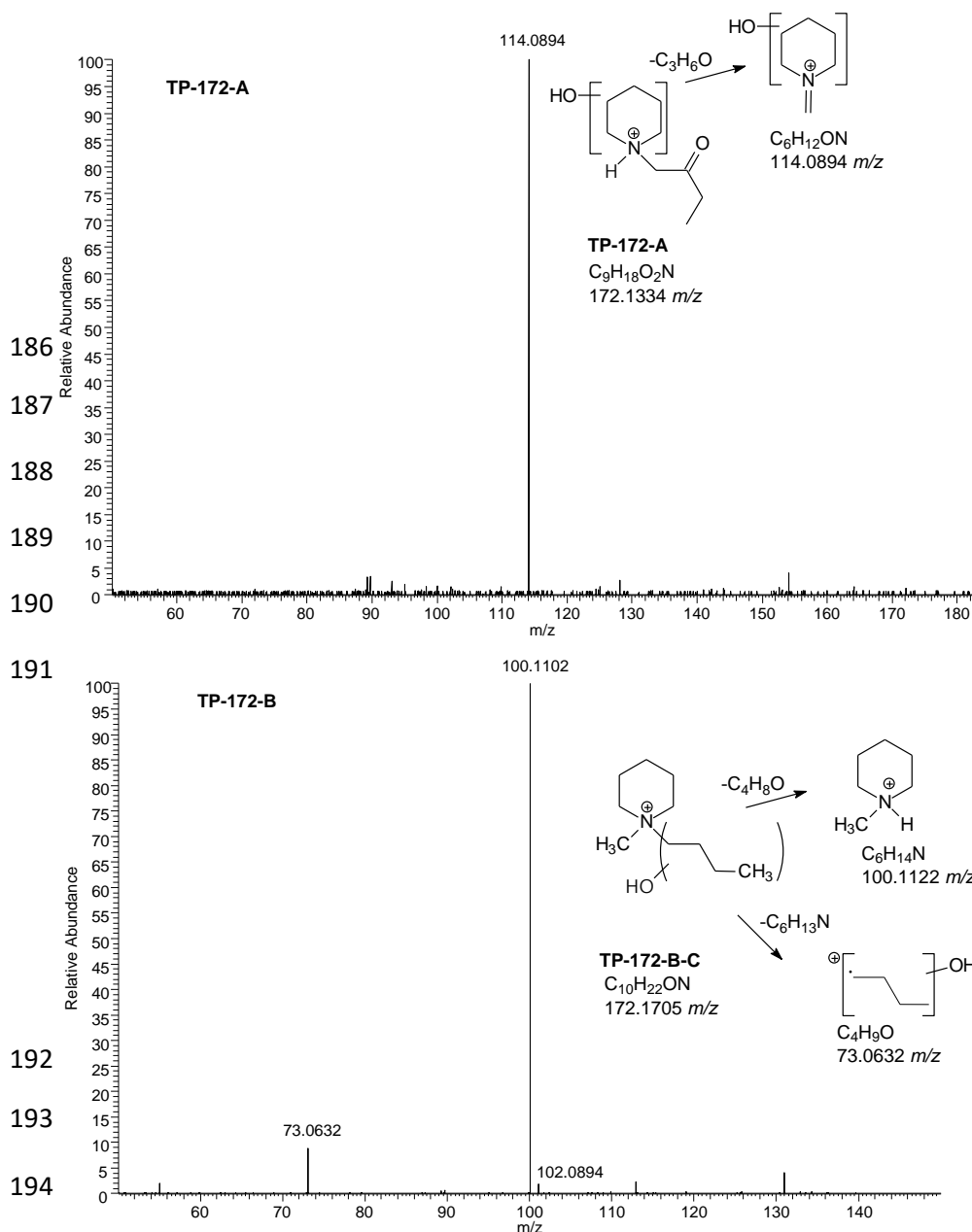
195   **Figure 3**. MS^2 spectra of TP-172-A and B and proposed fragmentation pathways followed by TPs

196   172.

197

198   Three abundant TPs were detected at 170.1547 *m/z* and represents a transformation of N-butal-N-

199   methylpiperidinium due to the subsequent oxidation of the hydroxyl group into carbonyl group. For

200   **TP-170-A** again the loss of C_4H_6O permits to locate the carbonyl group on the butyl chain.

201   Conversely, **TP-170-B** and **C** lose the unmodified chain, so allowing excluding an attack on the butyl

202   chain. Additionally, for **TP-170-B**, a CH_2/NH rearrangement takes place while chain fragmentation

occurs; for **TP-170-B**, the losses of CO and formaldehyde in MS^3 spectrum from the product ion at 114.0894 *m/z* is well matched with an oxidation on the methyl group (see Scheme 1).
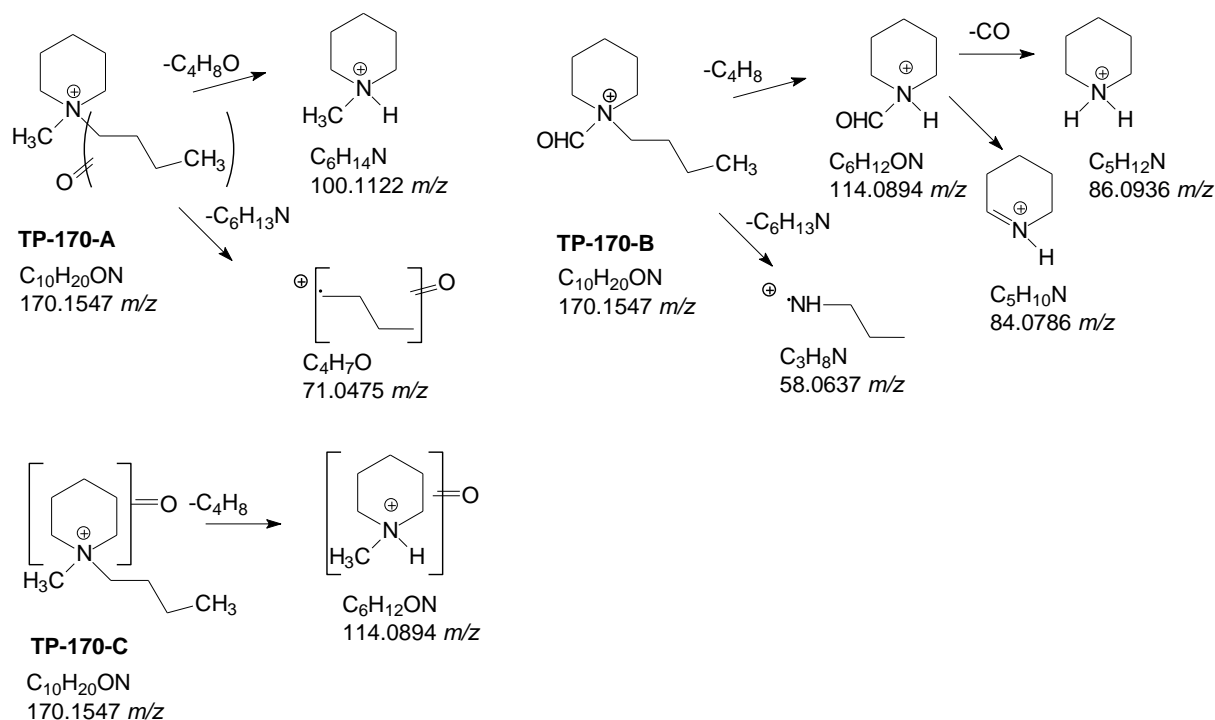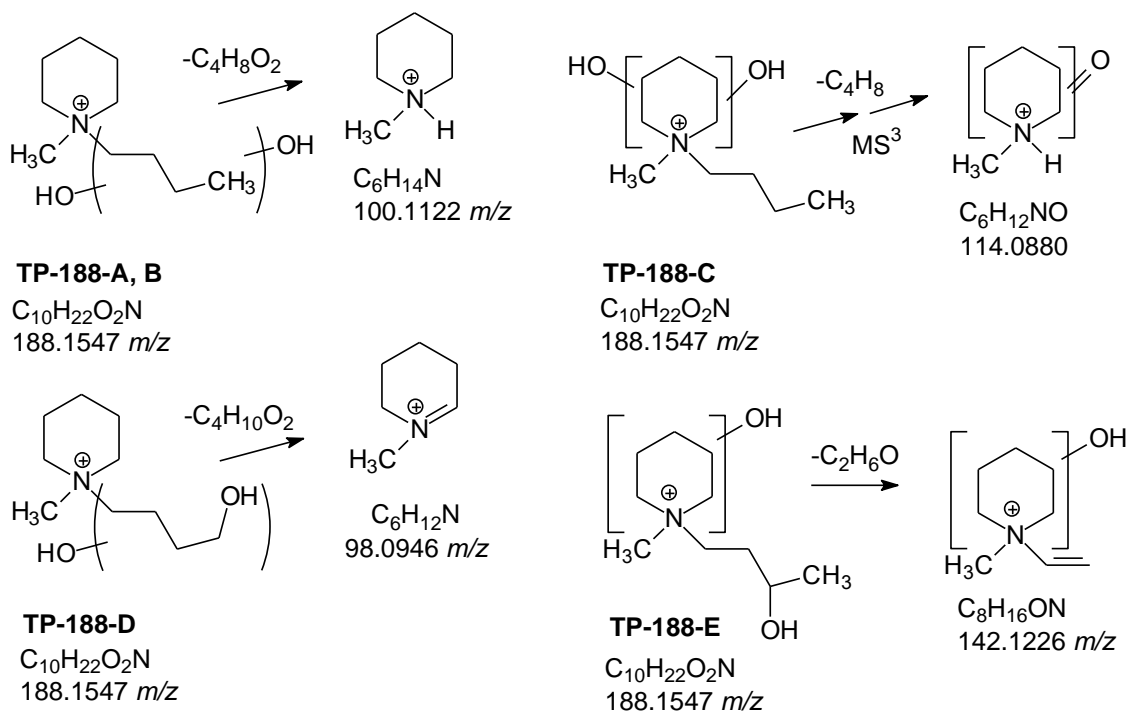

Scheme 1. Proposed fragmentation pathways followed by TPs 170.

A double hydroxylation accounts for the presence of six isobaric species at 188.1655 *m/z*. The fragmentation pathways of their molecular ions are shown in Scheme 2. **TP-188-A, B** and **D** hold both OH groups on the butyl chain, as proved by the loss of $C_4H_8O_2$. For **TP-188-D**, the combined losses of methanol and $C_3H_8O_2$, allowed to locate one of the two hydroxyl groups on C4 and the second one on C2 or C3. For **TP-188-C** the loss of C_4H_8 in MS^3 spectrum permits to exclude an attack on the butyl chain. For **TP-188-E** the loss of C_2H_6O combined with the absence of methanol loss permit assessing that one of the two hydroxyl groups is placed on C3. For **TP-188-F** the formation in MS^2 spectrum of the prominent ions $C_7H_{14}ON$ and $C_6H_{12}ON$ allows to locate the hydroxyl groups on C2 or C3, and the other one on the piperidine ring.
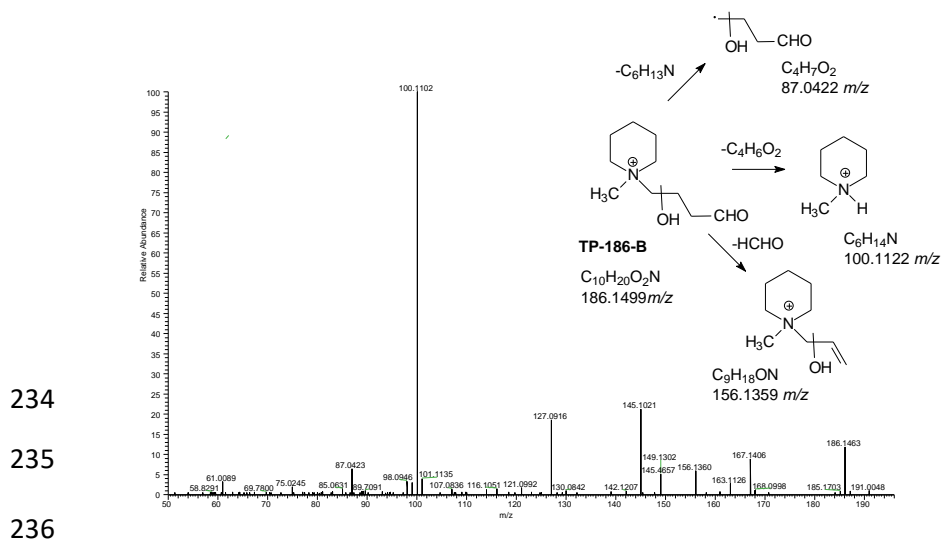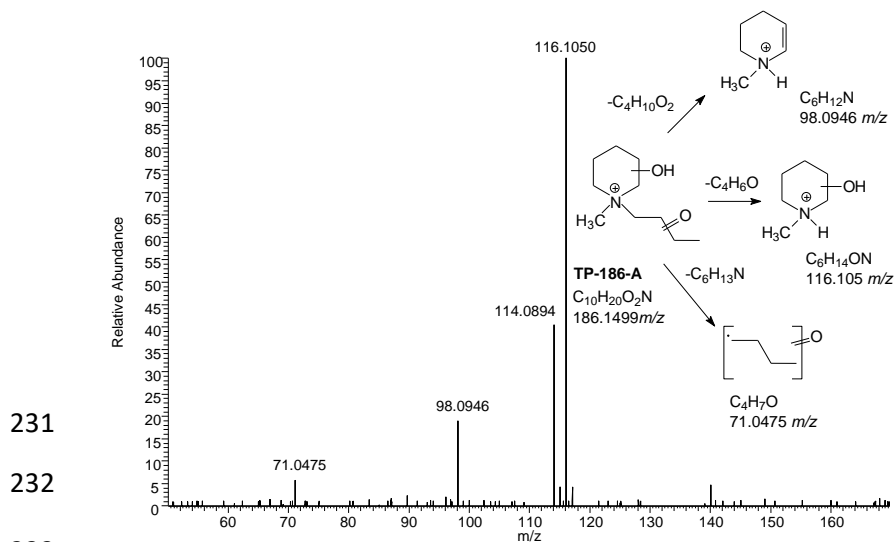
Scheme 2. Proposed fragmentation pathways followed by TPs 188.

Dihydroxylated BMPA is further oxidized to give two species at 186.1499 *m/z.* The mass-to-charge ratio of 186 potentially corresponds to a carboxylated product of BMPA or a product containing two functional groups (carbonyl and hydroxyl) [29]. For **TP-186-A**, the loss of C_4H_6O allows locating the carbonyl group on the butyl chain; the formation of the product ion at 98.0946 *m/z* permits to exclude the methyl hydroxylation and to locate the hydroxyl substituent on the piperidine ring. For **TP-186-B**, the formation of the ion at 100.1122 *m/z* as base peak allows to confine both hydroxylation and oxidation on the butyl chain; furthermore, the loss of formaldehyde agrees to locate the carbonyl group on C4 (see Figure 4).

**Figure 4**. MS^2 spectrum of TP-186-A and B and proposed fragmentation pathways followed by TPs 186.

A species at 184.1341 *m/z* (**TP-184**) was attributed to the bihydroxylated/bi-oxidized derivative. The formation of the product ion at 114.0894 *m/z* as base peak in MS^2 spectrum allows locating a carbonyl group on the butyl chain. MS^3 spectrum evidenced the loss of C_2H_4O that, combined with the absence of formaldehyde loss, endorsed locating the carbonyl group on C3. The formation of the product ion at 84.0790 *m/z* in MS^2 spectrum permits to place the other carbonyl group on the methyl substituent.

Six isobaric species at 202.1449 *m/z* are formed and attributed to trihydroxylated-oxidized compounds. Key fragmentation pathways are collected in Scheme 3. **TP-202-A** and **F** share the product ion at 114.0894 *m/z*, allowing to confine two of the three substituents on the butyl chain.
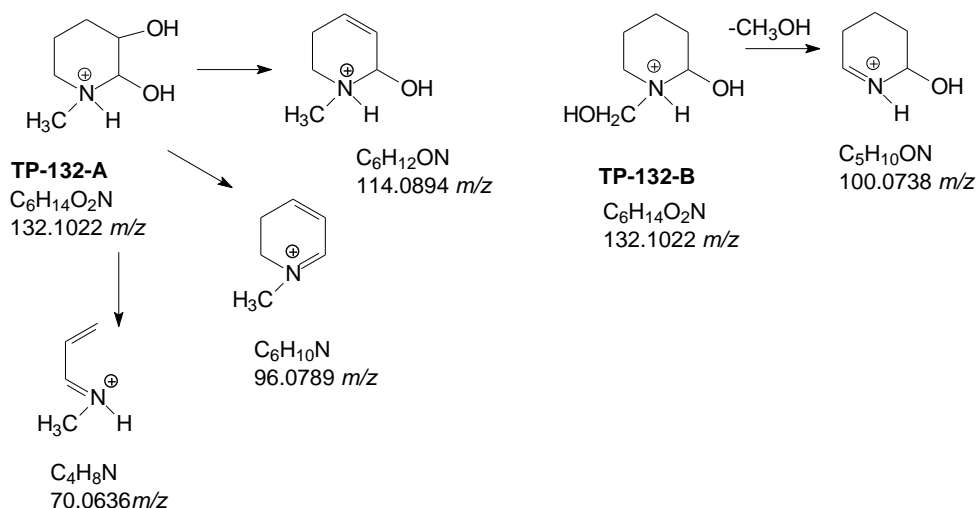
12

249 Furthermore, **TP-202-F** holds the structural diagnostic ion at 86.0947 *m/z*, attributed to the

250 piperidine moiety, so implying that the oxidation had involved the methyl group. Therefore, **TP-202-**

251 **A** holds necessarily the carbonyl group on the piperidine ring. **TP-202-B** exhibits the structural-

252 diagnostic loss of $C_2H_4O_2$ in MS^2 spectrum, so permitting to locate both the carbonyl group and one

253 of the two OH substituents on C3 and 4. For **TP-202-C** the formation of the product ion at 100.1102

254 *m/z* allows to exclude an involvement of the piperidine ring and to consider the three groups on the

255 butyl chain; the losses of $C_4H_6O_3$ and C_2H_6O permit to locate the groups on C1, 2 and 4. **TP-202-D**

256 holds only an OH group on the chain, due to the loss of C_4H_8O. For **TP-202-E** any structural diagnostic

257 ions were formed.
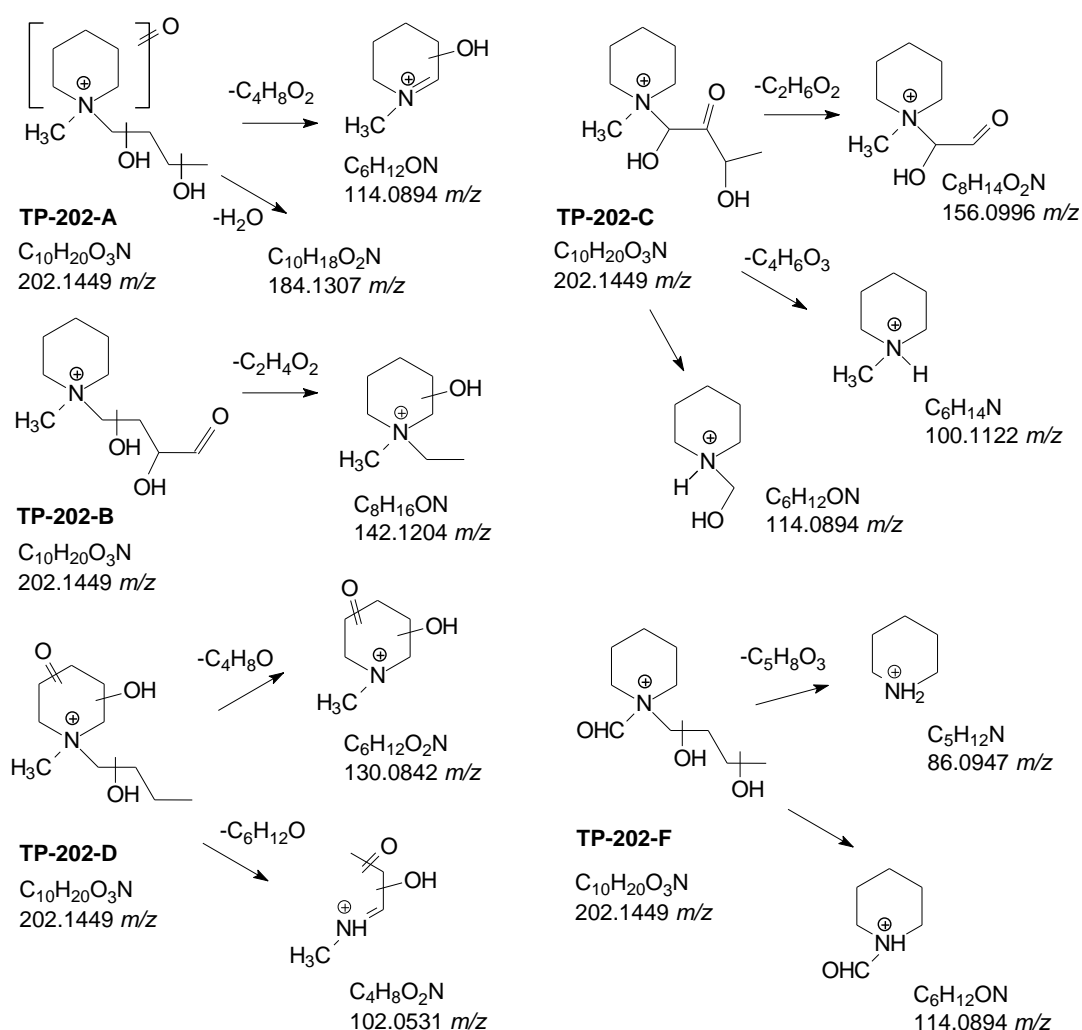
Scheme 3. Proposed fragmentation pathways followed by TPs 202.

261 A TP with 166.1234 *m/z* and empirical formula $C_{10}H_{16}ON$ is well matched with the formation of three

262 new unsaturations and the presence of a hydroxyl group. MS^2 key ions suggest that only one of the

three unsaturations and the hydroxyl group are confined on the butyl chain. The loss of C_4H_8O and C_4H_6O support this attribution (see comparison with parent molecule).

Two isobaric species with 132.1022 *m/z* were detected and attributed to dihydroxylated methyl piperidine. **TP-132-A** holds the two OH groups on the ring in C1 and C2, as assessed by the formation of the product ion at 70.0792 *m/z* in MS^2 spectrum, while **TP-132-B** has an hydroxyl group on the methyl and the other one on C1, as assessed by the loss of methanol and by the formation of ion at 70.0792 *m/z* (see Scheme 4).

TP-132-A
$C_6H_{14}O_2N$
132.1022 *m/z*

$C_6H_{12}ON$
114.0894 *m/z*

$C_6H_{10}N$
96.0789 *m/z*

C_4H_8N
70.0636 *m/z*

-CH$_3$OH

TP-132-B
$C_6H_{14}O_2N$
132.1022 *m/z*

$C_5H_{10}ON$
100.0738 *m/z*

Scheme 4. Proposed fragmentation pathways followed by TPs 132.

A TP with 100.1121 *m/z* was detected and attributed to N-methyl-piperidinium, in agreement with literature data [29], and was confirmed by injection of a standard solution. N-methylpiperidinium detected during the degradation process may be generated *via* the elimination of the oxidized butyl side chain.

Two isobaric species with 116.1071 *m/z* and empirical formula $C_6H_{14}ON$, well-matched with N-hydroxylmethylpiperidinium were detected (**TP-116-A** and **B**). For **TP-116-A** a single product ion was generated at 98.0946 *m/z*, while for **TP-116-B** the losses of C_2H_6 and C_3H_6O permitted us to locate the OH group on the ring in para position.

A species with 114.0915 *m/z* and empirical formula $C_6H_{12}ON$ was formed. The loss of formaldehyde in MS^2 spectrum allows to locate the carbonyl group on the methyl substituent; therefore, **TP-114** matches with N-formylpiperidinium.

A TP with 118.0864 *m/z* was detected as well and attributed to the bihydroxylated piperidinium. No MS^2 spectra are available.

A further reduction occurred to form 98.0806 *m/z* (N-methyl- 1,4-tetrahydropyridinium) and the demethylated derivative (84 *m/z*, 1,4-tetrahydropyridinium).

14

Compound with 88.0756 *m/z* and empirical formula $C_4H_{10}ON$ (**TP-88**) could be formed through the ring opening and could be attributed to the aminobutyl chain containing a carbonyl group. No MS^2 ions are available to elucidate the structure.

The overall detected compounds could be formed through the transformation pathways summarized in Scheme 5.
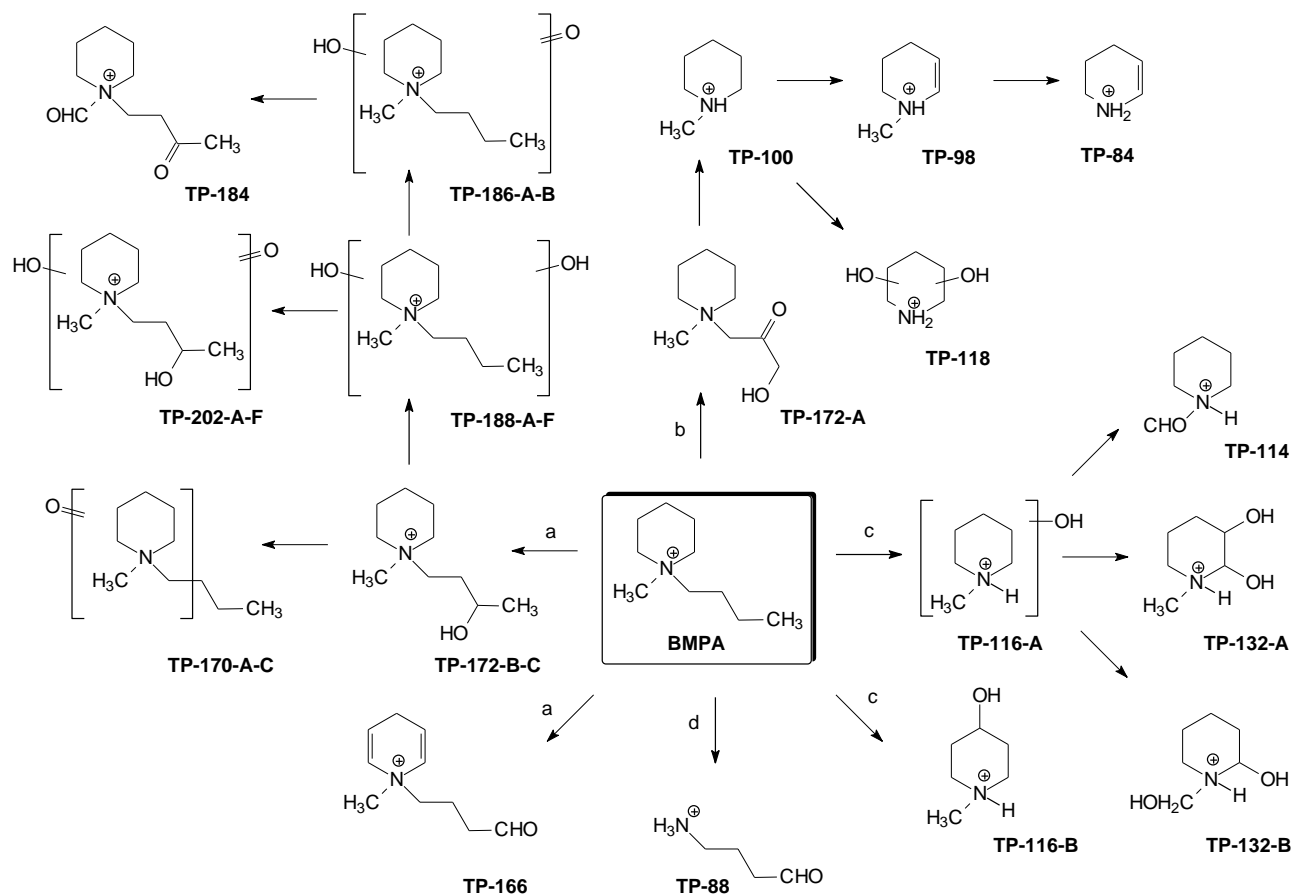
Scheme 5. Proposed transformation pathways followed by BMPA.

Four different transformation pathways are involved. Pathway **a** proceeds throught the hydroxylation and/or oxidation of the butyl chain, with the formation of **TP-172-B-C** derivatives that are then subjected to oxidation (**TP-170-A-C**) or further hydroxylation/oxydation (**TP-188**, **TP-186**). The pathways **b** and **c** imply respectively the chain shortening and the detachment of butyl chain with hydroxylation of the ring, whereas for the pathway **d** the formation of a TP arising from the ring opening is observed.

15

BMPA mineralization and acute toxicity

Figure 5 shows that BMPA in the presence of TiO_2 completely disappears within 45 min, while most of TOC disappeared within 2h. At that time, almost all the recognized TPs were degraded themselves. Then, complete mineralization was achieved within 4h.
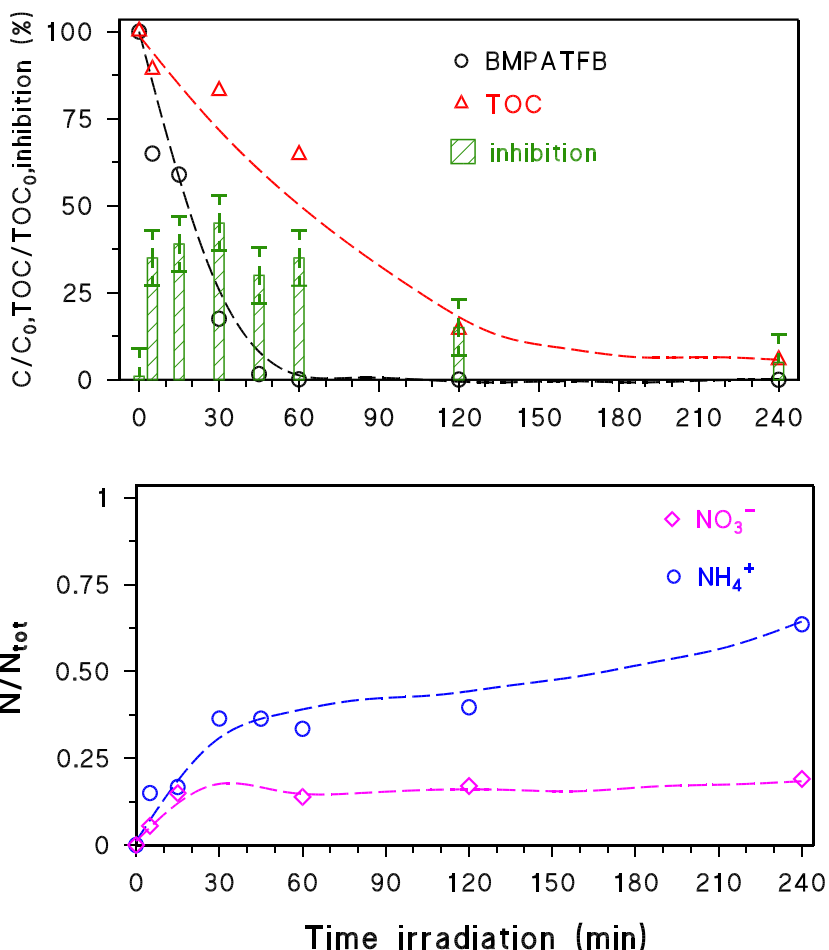
Figure 5. top) BMPA disappearance curve, TOC and acute toxicity; bottom) inorganic ions release for BMPA during the photocatalytic treatment.

BMPA is a non-toxic compound [30] but exhibited an increase of toxicity from 5 min onward. A first peak of toxicity was achieved at 5 min (35% inhibition) and then decrease to 5% at 15 min. This behavior can be attributed to the early formed TPs, namely **TP-188-B**, **TP-188-F**, **TP-130** and **TP-170-C**. Then, toxicity increased again and level off at 30% inhibition from 30 to 120 min of irradiation. Many TPs are formed at 30 min, but the most important should be **TP-170 A**, **TP-132-A**, **TP-186-A**, **TP-116-B** and **TP-84**. However, at 120 min the only TPs still present were **TP-118** and **TP-184**. Then, toxicity decreased to zero within 240 min of irradiation; at that time, complete mineralization was achieved.

321 Nitrogen was mainly released as ammonium ions (70%) and in a lesser extent to nitrate ion (20 %)

322 in agreement with literature data [31]; the stoichiometric amount was achieved after 240 min. At

323 that time, also TOC is almost zero. No nitrite traces were detected under the employed experimental

324 conditions.

325

326

327 **CONCLUSIONS**

328

329 In the present study, a method combining HPLC and LTQ-Orbitrap MS was established and used to

330 identify BMPA transformation products. Thirty-two TPS were found and identified by their

331 fragmentation patterns and accurate mass measurements. Twenty-one metabolites were related to

332 chains oxidation/hydroxylation, one degradant was related to chain shortening, seven TPs are

333 formed through the detachment of butyl chain, two transformation products were due to the

334 combined detachment of butyl and methyl chains, and one degradant was related to piperidine ring-

335 cleavage. This study provided useful information in understanding the transformation mechanism

336 of BMPA clearly demonstrating that HPLC/LTQ-Orbitrap MS analysis can serve as an important

337 platform by which to obtain the intermediates profiles of new products.

338

344

345

REFERENCES

[1] Seddon KR. Ionic Liquids for Clean Technology. *J Chem Technol Biotechnol* 1997;68:351-356.

[2] Stepnowski P, Zaleska A. Comparison of different advanced oxidation processes for the degradation of room temperature ionic liquids. *J Photochem Photobiol A* 2005;170:45-50.

[3] Kralisch D, Stark A, Korsten S, Kreisel G, Ondruschka B. Energetic, environmental and economic balances: spice up your ionic liquid research efficiency. *Green Chem* 2005;*7*:301–309.

[4] Banić N, Vraneš M, Abramović B, Csanádi J, Gadžurić S, Thermochromism, stability and thermodynamics of cobalt(II) complexes in newly synthesized nitrate based ionic liquid and its photostability. *Dalton Trans*. 2014;43:15515 -15525.

[5] Pham TPT, Cho CW, Yun YS, Environmental fate and toxicity of ionic liquids: A review. *Water Research* 2010;44:352 – 372.

[6] Calza P, Vione D, Fabbri D, Aigotti R, Medana C. Imidazolium-based ionic liquids in water: Assessment of photocatalytic and photochemical transformation. *Environ Sci Technol* 2015;49:10951-10958.

[7] Calza P, Noè G, Fabbri D, Santoro V, Minero C, Vione D, Medana C. Photoinduced transformation of pyridinium-based ionic liquids, and implications for their photochemical behavior in surface waters. *Water Research* 2017; doi: 10.1016/j.watres.2017.05.064.

[8] Stolte S, Steudte S, Igartua A, Stepnowski P. The biodegradation of ionic liquids–the view from a chemical structure perspective. *Curr. Org. Chem*. 2011;15: 1946–1973.

[9] Czerwicka M, Stolte S, Müller A, Siedlecka EM, Gołebiowski M, Kumirska J, Stepnowski P. Identification of ionic liquid breakdown products in an advanced oxidation system. *J Hazard Mater* 2009;171:478–483.

[10] Richardson SD, Ternes TA. Water analysis: emerging contaminants and current issues. *Anal. Chem*. 2014;86:2813–2848.

[11] Munos M, Dominguez CM, de Pedro ZM, Quintanilla A, Casas JA, Rodriguez JJ. Ionic liquids break down by Fenton oxidation. *Catalysis Today* 2015;240:16-21.

[12] Pieczynska A, Ofiarska A, Borzyszkowska AF, BiałkBielinska A, Stepnowski P, Stolte S, Siedlecka E M. A comparative study of electrochemical degradation of imidazolium and pyridinium ionic liquids: A reaction pathway and ecotoxicity evaluation. *Sep. Purif Technol* 2015;156,:522-534.

[13] Siedlecka E M, Stolte S, Gołębiowski M, Nienstedt A, Stepnowski P, Thöming J. Advanced oxidation process for the removal of ionic liquids from water: The influence of functionalized side chains on the electrochemical degradability of imidazolium cations. *Sep Purif Technol* 2012;101: 26-33.

[14] Itakura T, Hirata K, Aoki M, Sasai R, Yoshida H, Itoh H. Decomposition and removal of ionic liquid in aqueous solution by hydrothermal and photocatalytic treatment. *Environ Chem Lett* 2009;7:343-345.

378   [15] Siedlecka E M, Stepnowski P. The effect of alkyl chain length on the degradation of alkylimidazolium-
379   and pyridinium-type ionic liquids in a Fenton-like system. *Environ Sci Pollut Res* 2009;16:453–458.

380   [16] Calza P, Fabbri D, Noè G, Santoro V, Medana C. Assessment of the photocatalytic transformation of
381   pyridinium-based ionic liquids in water, submitted to J. Hazard. Mat

382   [17] Banic N, Abramovic B, Sibul F, et al. Advanced oxidation processes for the removal of [bmim][Sal] third
383   generation ionic liquids: effect of water matrices and intermediates identification. *RSC Adv* 2016;6:52826-
384   52837.

385   [18] Rout A, Venkatesan KA, Antony MP, Rao PRV. Comparison in the extraction behavior of uranium(VI) from
386   nitric acid medium using CHON based extractants, monoamide, malonamide, and diglycolamide, dissolved in
387   piperidinium ionic liquid. *Sep Sci Technol* 2016;51(3):474-484.

388   [19] Priya S, Arijit Sengupta, Jayabuna Sk, Adya VC. Piperidinium based ionic liquid in combination with
389   sulphoxides: Highly efficient solvent systems for the extraction of thorium. *Hydrometallurgy* 2016;164:111–
390   117.

391   [20] Wlazło M, Ramjugernath D, Naidoo P, Domańska U. Effect of the alkyl side chain of the 1-
392   alkylpiperidinium-based ionic liquids on desulfurization of fuels. *J Chem Thermodyn* 2014;732:31–36.

393   [21] Alinezhad H, Vafaeezadeh M, Hashemi MM. Formation of a catalytically active intermediate for oxidation
394   in H_2O_2/ionic liquid system: experimental and theoretical investigations. *Res Chem Intermediat*
395   2017;43:2615–2625.

396   [22] Hayyan M, Mjalli FS, Hashim MA, AlNashef IM, Al-Zahrani SM, Chooi KL. Long term stability of superoxide
397   ion in piperidinium, pyrrolidinium and phosphonium cations-based ionic liquids and its utilization in the
398   destruction of chlorobenzenes. *J Electroanal Chem* 2012;664:26–32.

399   [23] Szymczak J, Legeai S, Michel S, Diliberto S, Stein N, Boulanger C. Electrodeposition of stoichiometric
400   bismuth telluride Bi_2Te_3 using a piperidinium ionic liquid binary mixture, *Electrochim. Acta* 2014;137:586-594.

401   [24] Yuan LX, Feng JK, Ai XP, Cao YL, Chen SL, Yang HX. Improved dischargeability and reversibility of sulfur
402   cathode in a novel ionic liquid electrolyte. *Electrochem Commun* 2006;8:610614.

403   [25] Neumann J, Steudte S, Cho CW, Thöming J, Stolte S. Biodegradability of 27 pyrrolidinium, morpholinium,
404   piperidinium, imidazolium and pyridinium ionic liquid cations under aerobic conditions. *Green Chem*
405   2014;16:2174-2184.

406   [26] Pretti C, Renzi M, Focardi S E, et al. Acute toxicity and biodegradability of N-alkyl-N-methylmorpholinium
407   and N-alkyl-DABCO based ionic liquids. Ecotoxicol. *Ecotoxicol Environ Saf* 2011;74:748–753.

408   [27] Jordana A, Gathergood N. Biodegradation of ionic liquids – a critical review. *Chem Soc Rev* 2015;44:8200-
409   8237.

410   [28] Ionic Liquids Market Size And Forecast By Application, By Region And Trend Analysis From 2014 To 2025.
411   Research and Markets Report, Dublin 2014.

412 [29] Zhou H, Lv P, Shen Y, Wang J, Fan J. Identification of degradation products of ionic liquids in an ultrasound

413 assisted zero-valent iron activated carbon microelectrolysis system and their degradation mechanism. *Water*

414 *Research* 2013;47: 3514-3522.

415 [30] Ventura SPM, Marques CS, Rosatella AA, Alfonso CAM, Goncalves F, Coutinho JAP. Toxicity assessment

416 of various ionic liquid families towards *Vibrio fischeri* marine bacteria. *Ecotox Environ Safe* 2012;76:162-

417 168.

418 [31] Calza P, Pelizzetti E, Minero C. The fate of the organic nitrogen in photocatalysis. An overview. *J Appl*

419 *Electrochem* 2005;35:665-673.

420

421

422

423

424   **Table 1**. [M+H]$^+$ and MS^2 product ions for compound BMPA.

[M+H]$^+$	Name	Δmmu	t$_R$	[M+H]$^+$	Name	Δmmu	t$_R$
156.1753 $C_{10}H_{22}N$	BMPA	0.544	17,45	202.1449 $C_{10}H_{20}O_3N$	TP-202-A	1.07	5.21
172.1334 $C_9H_{18}O_2N$	TP-172-A	0.695	8.21		TP-202-B	1.07	7.69
172.1705 $C_{10}H_{22}ON$	TP-172-B	0.759	10.06		TP-202-C	1.07	8.93
172.1705 $C_{10}H_{22}ON$	TP-172-C	0.759	12.54		TP-202-D	1.07	9.55
166.1234 $C_{10}H_{16}ON$	TP-166	0.729	9.41		TP-202-E	1.07	10.17
170.1547 $C_{10}H_{20}ON$	TP-170-A	0.679	10.72		TP-202-F	1.07	12.03
	TP-170-B	0.679	11.34	132.1022 $C_6H_{14}O_2N$	TP-132-A	0.315	3.72
	TP-170-C	0.679	15.04		TP-132-B	0.315	5.55
188.1655 $C_{10}H_{22}O_2N$	TP-188-A	0.865	7.65	116.1071 $C_6H_{14}ON$	TP-116-A	0.159	5.04
	TP-188-B	0.865	9.51		TP-116B	0.159	6.28
	TP-188-C	0.865	11.38	114.0915 $C_6H_{12}ON$	TP-114	0.169	4.34
	TP-188-D	0.865	11.98	100.1121 $C_6H_{14}N$	TP-100	0.004	9.17
	TP -188-E	0.865	14.46	118.0864 $C_5H_{12}O_2N$	TP-118	0.155	4.40
	TP -188-F	0.865	15.04	98.0964 $C_6H_{12}N$	TP -98	0.014	6.98
186.1499 $C_{10}H_{20}O_2N$	TP-186-A	0.975	6.52	88.0756 $C_4H_{10}oN$	TP-88	-0.131	1.25
	TP-186-B	0.975	10.23	88.0756 $C_4H_{10}oN$	TP-88	-0.131	1.25
184.1341 $C_{10}H_{18}O_2N$	TP-184	0.935	7.17				